Metabolic alterations derived from absence of Two-Pore Channel 1 at cardiac level

Vanessa García-Rúa[1,†], Sandra Feijóo-Bandín[1,†,*], María García-Vence[1,†], Alana Aragón-Herrera[1], Susana B Bravo[2], Diego Rodríguez-Penas[1], Ana Mosquera-Leal[1], Pamela V Lear[3], John Parrington[3], Jana Alonso[2], Esther Roselló-Lletí[4], Manuel Portolés[4], Miguel Rivera[4], José Ramón González-Juanatey[1] and Francisca Lago[1]

[1]*Cellular and Molecular Cardiology Research Unit and Department of Cardiology, Institute of Biomedical Research and University Clinical Hospital, 15706, Santiago de Compostela, Spain*

[2]*Laboratory of Proteomics, Institute of Biomedical Research and University Clinical Hospital, 15706, Santiago de Compostela, Spain*

[3]*Department of Pharmacology, University of Oxford, Oxford, UK*

[4]*La Fe University Hospital, 46026, Valencia, Spain*

**Corresponding author (Email, sandra.feijoo@gmail.com)*

[†]These authors contributed equally to the work.

Two-pore channels (TPCs or TPCNs) are novel voltage-gated ion channels that have been postulated to act as Ca^{2+} and/or Na^{+} channels expressed exclusively in acidic organelles such as endosomes and lysosomes. TPCNs participate in the regulation of diverse biological processes and recently have been proposed to be involved in the pathophysiology of metabolic disorders such as obesity, fatty liver disease and type 2 diabetes mellitus. Due to the importance of these pathologies in the development of cardiovascular diseases, we aimed to study the possible role of two-pore channel 1 (TPCN1) in the regulation of cardiac metabolism. To explore the cardiac function of TPCN1, we developed proteomic approaches as 2-DE-MALDI-MS and LC-MALDI-MS in the cardiac left ventricle of TPCN1 KO and WT mice, and found alterations in several proteins implicated in glucose and fatty acid metabolism in TPCN1 KO *vs.* WT mice. The results confirmed the altered expression of HFABP, a key fatty acid transport protein, and of enolase and PGK1, the key enzymes in the glycolytic process. Finally, *in vitro* experiments performed in neonatal rat cardiomyocytes, in which TPCN1 was silenced using siRNAs, confirmed that the downregulation of TPCN1 gene expression increased 2-deoxy-D-[3H]-glucose uptake and GLUT4 mobilization into cell peripherals in cardiac cells. Our results are the first to suggest a potential role for TPCNs in cardiac metabolism regulation.

[García-Rúa V, Feijóo-Bandín S, García-Vence M, Aragón-Herrera A, Bravo SB, Rodríguez-Penas D, Mosquera-Leal A, Lear PV, Parrington J, Alonso J, Roselló-Lletí E, Portolés M, Rivera M, González-Juanatey JR and Lago F 2016 Metabolic alterations derived from the absence of Two-Pore Channel 1 (TPCN1) at cardiac level. *J. Biosci.* **41** 643–658]

1. Introduction

Two-pore channels (TPCs or TPCNs) are novel members of the voltage-gated ion channel superfamily originally sequenced from a rat kidney-cell cDNA library in 2000 as a result of their structural homology with voltage-gated Na^{+} and Ca^{2+} channels (Ishibashi *et al.* 2000). They were called TPCNs because they contain two repeats of a 6 trans-membrane pore-forming domain, being an intermediate form between the endo-lysosomal transient receptor potential channels (TRPs, one domain repeat) and the voltage-gated Ca^{2+} channels (VGCCs, four domain repeats) (Ishibashi

Keywords. 2-DE-MALDI-MS; cardiomyocytes; knockout; LC-MALDI-MS; TPCN1

Supplementary materials pertaining to this article are available on the Journal of Biosciences Website.

DOI: 10.1007/s12038-016-9647-4

Published online: 23 November 2016

et al. 2000; Zhu *et al.* 2010). The TPCN gene is widespread across the animal kingdom, which is indicative of its phylogenetic and functional relevance, and has undergone multiplication with most species possessing either two (TPCN1 and TPCN2 in humans and rats) or three (TPCN1, TPCN2 and TPCN3 in sea urchin) TPCN genes, TPCN1 and TPCN2 being the most universal isoforms (Brailoiu *et al.* 2009).

TPCNs are expressed exclusively in acidic organelles such as endosomes and lysosomes in animals (Brailoiu *et al.* 2009; Calcraft *et al.* 2009; Zong *et al.* 2009) and vacuoles in plants (Peiter *et al.* 2005), and they have been firstly described as Ca^{2+} release channels activated through the second messenger nicotinic acid adenine diphosphate (NAADP) (Brailoiu *et al.* 2009; Calcraft *et al.* 2009; Ruas *et al.* 2010; Dionisio *et al.* 2011; Pereira *et al.* 2014). However, other authors have also demonstrated that TPCNs are Na^{+}-selective channels activated by phospho-inositol 3,5-diphosphate ($PI(3,5)P_2$) (Wang *et al.* 2012; Cang *et al.* 2013) and regulated via mammalian target of rapamycin (mTOR) (Cang *et al.* 2013). These findings are in agreement with the TPCN structural homology with voltage-gated Na^{+} and Ca^{2+} channels (Ishibashi *et al.* 2000), suggesting that they can act as both Na^{+} and Ca^{2+} channels.

Several studies have shown that TPCN1 and/or TPCN2 activation participate in the regulation of diverse biological processes, including cell differentiation (Aley *et al.* 2010; Notomi *et al.* 2012; Zhang *et al.* 2013; Parrington and Tunn 2014), acrosome exocytosis (Arndt *et al.* 2014), cytokinesis (Horton *et al.* 2015), angiogenesis (Favia *et al.* 2014) and, interestingly, autophagy (Lu *et al.* 2013) and muscle contraction (Tugba Durlu-Kandilci *et al.* 2010), both of them being mechanisms of special relevance in tissues highly specialised and differentiated as is the case of the cardiac tissue (Terman and Brunk 2005). Moreover, different studies performed in mice lacking TPCN genes have proved the implication of these novel channels in the pathophysiology of metabolic disorders such as obesity (Lear *et al.* 2014), fatty liver disease (Grimm *et al.* 2014) and type 2 diabetes mellitus (T2DM) (Tsaih *et al.* 2014), all of them conditions that are well known to be implicated in the development of metabolic syndrome and in the pathophysiology of cardiovascular diseases (Bastien *et al.* 2013; Bang and Cho 2015; Grundy 2015).

In a previous study, we showed the upregulation of both TPCN1 and TPCN2 genes in left ventricular (LV) tissue of patients with heart failure (Garcia-Rua *et al.* 2012), which is a pathological state characterised by several metabolic alterations, ranging from changes in substrate use to mitochondrial dysfunction, ultimately resulting in ATP deficiency and impaired contractility (Wang *et al.* 2014). Here we aimed to explore the possible role of these novel voltage-gated ion channels in the cardiac physiology, focusing on the identification of candidate proteins that could mediate TPCN1 implication in cardiac metabolism regulation. To this purpose, we developed proteomics approaches to characterise the cardiac proteome of mice lacking the TPCN1 gene by mass spectrometry techniques, and *in vitro* approaches to determine the implication of the absence of TPCN1 in energy substrates uptake by cardiomyocytes.

2. Material and methods

All reagents were obtained from Sigma Aldrich (US) unless otherwise stated.

2.1 *Ethics statement*

The study protocol was approved by the Galician Clinical Research Ethics Committee (2007/304). All animals were maintained and killed following protocols approved by the Animal Care Committee of the University of Santiago de Compostela in accordance with European Union Directive 2010/63.

2.2 *Animals*

Hearts from TPCN1 knockout (KO) male mice and their corresponding wild-type (WT) mice of the same age (9 months), sex (male) and background (C57Bl/6;129) were a kind gift from Dr John Parrington and Dr Pamela Lear (Department of Pharmacology, Oxford University, UK). The TPCN1 KO mouse line (showing no detectable expression of either TPCN1A or TPCN1B, a newly identified alternative transcript (Ruas *et al.* 2014)) has been previously described (Ruas *et al.* 2014).

Neonatal (1- to 3-day-old) Sprague–Dawley rats were killed by cervical dislocation, and their hearts were used for establishment of primary cardiomyocyte cultures (see below).

2.3 *Protein extraction*

Proteomic analysis and two-dimensional electrophoresis (2-DE) Western blot were conducted using LV from TPCN1 KO and WT mice. LVs were dissected from the hearts (n=3) and lyophilized. The powder was resuspended in 2-DE extraction buffer (65 mM DTT, 65 mM CHAPS, 5 M urea, 2 M thiourea, 0.15 M NDSB-256, 200 nM tributylphosphine, 100 nM NaF, 1 M Na_3VO_4, and 1 M benzamidine) and stored at –80°C until further use. The resuspended protein was centrifuged at 13000*g* for 5 min and subsequently quantified prior to use (RC DC Protein Assay, BioRad Lab, US).

One-dimensional electrophoresis (1-DE) Western blot was performed using cardiac LV tissue from TPCN1 KO and WT mice. LV tissue was lysed with Triton X-100 1%

buffered in 50 mM Tris-HCl, 150 mM NaCl, 5 mM ethylenediaminetetraacetic acid (EDTA), 0.1 M NaF, 1 mM phenylmethylsulphonylfluoride (PMSF), 10 μg/mL leupeptin, 10 μg/mL aprotinin, 10 μg/mL trypsin inhibitor and 1 mM Na_3VO_4. The lysate was subsequently centrifuged at 13000*g* for 16 min at 4°C and quantified prior to use (RC DC Protein Assay, BioRad Lab, US).

2.4 *Isoelectric focusing and 2-DE*

Isoelectric focusing (IEF) was performed in pH 4-7 immobilized pH gradient (IPG) strips of 24 cm (GE Healthcare, UK). 500 μg of protein from LV of TPCN1 KO and WT mice independently was applied to each strip, and subjected to passive rehydration in 250 μL of 2-DE extraction buffer supplemented with ampholytes (0.1% servalyte 3–10, 0.05% servalyte 9-10 (SERVA, DE)) during 24 h after centrifugation at 13000*g* for 5 min. Passive rehydration was followed by active rehydration at 50 V during 12 h before IEF, performed in a Protean IEF Cell focusing unit (BioRad, USA) until 20000 V/total h were reached.

Subsequently to IEF, the IPG strips were equilibrated for 15 min in 4 M urea, 2 M thiourea, 50 mM Tris pH 6.8, 2% sodium dodecyl sulphate (SDS), 12 mM dithiothreitol (DTT) and 30% glycerol. SDS polyacrylamide gel electrophoresis (SDS-PAGE) was performed on 12% polyacrylamide gels using a Protean Plus Dodeca Cell (BioRad, USA) at 15 mA/gel for 12 h or until the dye front reached the bottom of the gel, at 18°C constant temperature.

The 2-DE gels were stained with Sypro Ruby (Lonza, CH) following manufacturer's instructions.

2.5 *Image acquisition and software analysis of 2-DE gels*

The Sypro Ruby stained 2-DE gels were scanned using a Typhoon fluorescence scanner (GE Healthcare, UK). The scanned images were processed using the Progenesis SameSpots software (Version 4.5) (Nonlinear Dynamics, NZ). Both manual and automatic alignment were used to align the images. All of the gels were compared, and the fold-changes (FC) and *p* values of all of the spots were calculated using the SameSpots software with 1-way ANOVA analysis. The differential protein expression was considered significant when the FC was at least 1.8 and the p value was <0.05.

2.6 *Tryptic digestion*

The digestion of the spots from 2-DE was manually performed according to the protocol of Shevchenko *et al.* (1996), with minor modifications. Briefly, the spots selected from representative 2-DE gels were excised and washed with a solution containing 50 mM NH_4HCO_3 and 50% MeOH (HPLC grade, Scharlau, ES). The proteins were reduced with 10 mM DTT in 50 mM NH_4HCO_3 and alkylated with 55 mM iodoacetamide in 50 mM NH_4HCO_3. Subsequently, the proteins were rinsed with 50 mM NH_4HCO_3 in 50% MeOH, dehydrated through the addition of acetonitrile (ACN) (HPLC grade, Scharlau, ES) and dried in a Speed Vac (Thermo Scientific, USA). Modified porcine trypsin (Promega, USA) was added to the dried gel slices at a final concentration of 20 ng/μL in 20 mM NH_4HCO_3, followed by incubation at 37°C for 16 h. The peptides were extracted three times by incubation in 40 μL of 60% ACN in 0.5% formic acid (HCOOH) for 20 min. The resulting peptide extracts were pooled, concentrated in a Speed Vac and stored at −20°C. Prior to 2-DE-MALDI-MS identification, the dried samples were dissolved in 4 μL of 20% ACN in 0.5% HCOOH.

In a separate experiment, 200 μg of the LV extracted protein from TPCN1 KO and WT mice was loaded onto a 10% SDS-polyacrylamide. 1-DE was conducted until the dye front was 3 mm into the resolving gel (Bonzon-Kulichenko *et al.* 2011; Perez-Hernandez *et al.* 2013; Roca-Rivada *et al.* 2015). The protein concentrate was visualized through Sypro Ruby fluorescent staining (Lonza, CH), and the protein digestion was assessed as described above. Prior to at a flow rate of 300 LC-MALDI-MS identification, the peptide mix was dissolved in 10–20 μL of 0.1 % HCOOH in 2% ACN (A solution).

2.7 *Protein identification through 2-DE/LC-MALDI-MS*

MALDI-MS analysis of the peptides digested from spots was performed by mixing equal volumes (0.5 μL) of peptide and matrix solution (3 mg of α-cyano-4-hydroxycinnamic acid (CHCA) dissolved in 1 mL of 50% ACN in 0.1% trifluoroacetic acid (TFA)). The mixture was deposited onto a 384 Opti-TOF MALDI plate (Applied Biosystems, USA) using the thin layer method. Separation of the resulting tryptic peptide mixtures from 1-DE electrophoresis was performed using nanoscale reversed-phase LC. The nanoLC Ultra 1D Plus (EKsigent, AB Sciex Boston, USA) was coupled to a MALDI-spotter (Eksigent, AB Sciex). The peptides mixtures were re-dissolved in A solution (0.1% HCOOH, 2% ACN) and injected into the trapping column (ChromXP nanoLC Trap column 350 μm id × 0.5 mm, ChromXP C18 3 μm 120 Å, AB Sciex) at a flow rate of 10 μl/min (0.1% HCOOH, 2% ACN). After 15 min, the trapped peptides were separated by reversed-phase chromatography on a nanocolumn (ChromXP nanoLC column 75 μm id × 15 cm, ChromXP C18 3 μm 120 Å, AB Sciex) at a flow rate of 300 mL/min in a linear elution gradient from 95% A solution to 60% B solution (90% ACN, 0.1% HCOOH) over 80 min, followed by an increase to 95% B solution over 5 min. The eluted peptides were mixed with a matrix solution containing 3 mg CHCA dissolved in 1 mL of 50% ACN in 0.1% TFA,

and 10 fmol/μL angiotensin I (as an internal standard) was deposited onto an Opti-TOF LC/MALDI insert (AB Sciex, USA) at a speed of one spot per 12 seconds.

MS data were obtained in an automated analysis loop using a 4800 MALDI-TOF/TOF Analyzer (Applied Biosystems, USA). The MS spectra were acquired in reflector positive-ion mode with a Nd:YAG, 355-nm wavelength laser, averaging 1000 laser shots, and at least three trypsin autolysis peaks were used as an internal calibration for peptides derived from spots and the 1296.685 angiotensin I peak for peptides separated by LC. All MS/MS spectra were performed after selecting precursors with a relative resolution of 300 (FWHM) and metastable suppression. The automated analysis of mass data was achieved using 4000 Series Explorer software V3.5. The MS and MS/MS spectra data from 2-DE were combined using GPS Explorer software v3.6 and Mascot software v2.1. (Matrix Science) to search against a non-redundant database (SwissProt release 56.0). The peptides and proteins from LC were identified using Protein Pilot software version 4.0.80.85 (AB Sciex, USA) with the Paragon Algorithm, and the MS/MS data were searched against the UniProt/Swiss-Prot database of protein sequences (July 2014; Swiss-Prot, Switzerland). The searches were restricted to *Mus musculus* taxonomy using carbamidomethyl cysteine as a fixed modification and oxidized methionine as a variable modification, with 30 ppm precursor tolerance, 0.35 Da MS/MS fragment tolerance and one missed cleavage. All spectra and database results were manually inspected using the aforementioned software. Proteins scores greater than 56 were accepted as significant ($p<0.05$), and a protein score CI% (Confidence Interval) greater than 98 was considered to be a positive identification. For MS/MS spectra, a total ion score CI% greater than 95 was considered to be a positive identification.

2.8 *Neonatal rat cardiomyocytes primary cultures*

Neonatal rat cardiomyocytes were cultured as previously described (González-Juanatey *et al.* 2003) and seeded at 50000 cells/cm^2.

2.9 *siRNA transfection*

The cardiomyocytes, 24 h after plating, were incubated for 6 h with 200 nM of small interfering RNA (siRNA) negative control (SIC 001, Sigma Aldrich) or 200 nM siRNAs targeting TPCN1 (SASI_Rn01_00107855 and SASI_Rn01_00107855_AS, Sigma Aldrich, USA) in conjunction with Thermo Scientific DharmaFECT 1 transfectant in Opti-MEM medium according to the manufacturer's instructions.

2.10 *Real-time quantitative PCR (RT-qPCR)*

RT-qPCR was performed on RNA extracted using the NucleoSpin Kit, according to the manufacturer's instructions (Macherey-Nagel, DE). For relative quantification, we performed a reverse-transcription reaction using 500 ng of RNA and the Transcriptor First Strand cDNA Synthesis kit (Roche, DE). RT-qPCR was performed using the master mix, specific primers and TaqMan-MGB probes provided by Roche: TPCN1: 68 bp, Assay Id 50591 RefSeq NM_139332 4, and 18S: 78 bp, Assay Id 502300 RefSeq XO1117. The amplification conditions were 95°C for 10 min, followed by 40 cycles of 95°C for 15 s and 60°C for 60 s. The results were analysed using MxPro v4 software (Stratagene, USA).

2.11 *Western blot analysis*

The protein extracted from TPCN1 KO and WT mice left ventricle was subjected to 2-DE Western blot analysis. 100 μg of protein was loaded onto pH 4-7 (heart-type fatty acid-binding protein (HFABP) and enolase) or 3-10 (phosphoglycerate kinase 1 (PGK1)) 7 cm IPG strips (GE Healthcare, UK). 2-DE was performed on 12% SDS-polyacrylamide gels. At the same time, we performed 1-DE SDS-PAGE/Western blot as previously described (González-Juanatey *et al.* 2003). We used antibodies against HFABP (Santa Cruz Biotechnology, USA), enolase (Santa Cruz Biotechnology, USA) and PGK1 (R&D systems, USA) according to manufacturer instructions. The membranes were subsequently incubated with a horseradish-peroxidase-conjugated secondary antibody (Santa Cruz Biotechnology, USA) and subjected to chemiluminescence detection (Millipore Corporate, USA). In all cases, densitometric analyses were performed using the UVP EC3 Imaging System (Ultra-Violet Products Ltd) and the Image J program (V1.43 q; Rasband 1997-2008).

2.12 *BODIPY-labelled fatty acid uptake*

After 48 h post-transfection, neonatal rat cardiomyocytes were treated with PBS containing 10 μM 4,4-difluoro-5-methyl-4-bora-3a,4a-diaza-s-indacene-3-dodecanoic acid (BODIPY 500/510 C1, C12; Life Technologies, USA) and 20 μM fatty acid-free BSA for 30 sec. Cells were also stained with propidium iodide (1 μM) to identify dead cells and analysed in a FACSCALIBUR flow cytometer (Becton Dickinson, USA) using the Cell Quest program.

2.13 *Glucose uptake assay*

After 48 h post-transfection, neonatal rat cardiomyocytes were serum-deprived for 2.5 h. Treatment for 1 h with

insulin (100 nM) was used as a positive control. The cells were washed twice in a glucose-free HEPES-buffered saline solution (140 mM NaCl, 5 mM KCl, 2.5 mM $MgSO_4$, 1 mM $CaCl_2$, and 20 mM HEPES, pH 7.4), and glucose uptake was determined as previously described using 2-deoxy-D-[3H] glucose (PerkinElmer, USA) (Feijóo-Bandín *et al.* 2013). Glucose uptake was measured using a Tri-Carb Liquid Scintillation Counter (Perkin Elmer, USA). Non-specific glucose uptake was determined in the presence of 10 µM cytochalasin B and subtracted from the data.

2.14 *Immunocytofluorescence labelling and confocal microscopy*

After 48 h post-transfection, neonatal rat cardiomyocytes were serum-deprived for 2.5 h and processed as previously described (Feijóo-Bandín *et al.* 2013) using anti-GLUT4 antibodies (Abcam, UK) at 1:100 dilution. Quantitative confocal microscopy was performed using a LeicaDMIRE2 confocal microscope (Leica, DE) and the software ImageJ was used to compare GLUT4 concentrations in the cell peripherals with those in the cytoplasm and perinuclear region as previously described (Feijóo-Bandín *et al.* 2013). A total of 108 cells were analysed.

2.15 *Statistical analysis*

All experiments were made at least with three biological replicates. For LC-MALDI-MS analysis, technical replicates were made using the same samples in a 30 min separation through the nanocolumn (data not shown). For 2-DE-MALDI-MS proteomic analysis, the statistical significance of the differences between mean values was determined with one-way ANOVA test using the SameSpots Version 4.5 software (Nonlinear Dynamics, UK). Comparison of mean values between two groups was assessed using the Student's *t*-tests, and FC respect to controls were assessed with Wilcoxon signed rank tests using the Prism V.5 (GraphPad Software, USA).

3. Results

3.1 *Proteomics analysis of LV from TPCN1 KO mice hearts using 2-DE-MALDI-MS*

An effective separation of cardiac LV proteome was obtained through 2-DE by applying a linear 4–7 pH gradient (in the first dimension) and using 12% SDS-polyacrylamide gels (in the second dimension), which adequately resolves proteins in the range of 10 to 150 kDa (figure 1). Software for statistical analysis of Sypro Ruby stained gels revealed

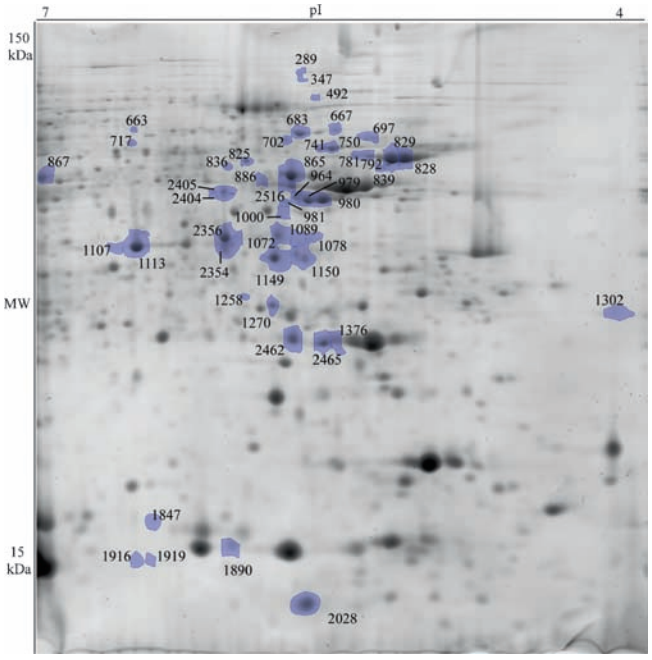

Figure 1. Representative 2-DE virtual map of the cardiac left ventricle from TPCN1 KO *vs.* WT mice. Three subjects per group were selected to develop the corresponding analysis using the SameSpots software. The proteins were separated over a pI range of 4 to 7 in the first dimension and on 12% SDS-polyacrylamide gels in the second dimension. The gels were stained with Sypro Ruby and 1072 protein spots were observed. The differentially expressed protein spots are numbered and were considered significant when the FC was at least 1.8 and the p value was <0.05. pI: isoelectric point, MW: molecular weight.

1072 protein spots, with 50 spots differentially regulated (49 upregulated and only 1 downregulated, $p<0.05$) in the cardiac LV from TPCN1 KO *vs*. WT mice (supplementary table 1).

All of the 50 but 3 spots were identified by MALDI-MS, 29 of them represented in just 1 spot (supplementary tables 1 and 2), and 17 represented in more than 1 spot (supplementary table 1).

The different proteins identified by 2-DE-MALDI-MS in cardiac LV of TPCN1 KO with altered expression *vs.* WT mice were further classified using the NCBI, PantherDB, and Uniprot databases into 5 groups based on their biological function (figure 2) (supplementary tables 1 and 2): (1) proteins associated with metabolic processes, subdivided into 4 different subgroups: glycolysis, lipid metabolism, tricarboxylic acid cycle (TCA) and respiratory electron transport chain; (2) proteins associated with muscle contraction; (3) proteins associated with cytoskeleton organization; (4) transport proteins and (5) the chaperone protein stress-70 protein (supplementary table 2).

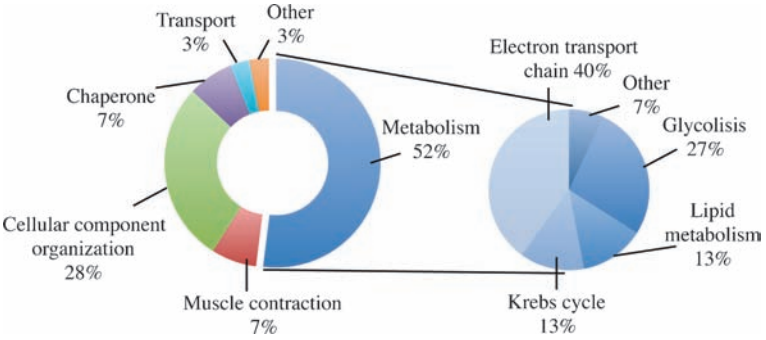

Figure 2. Results from 2-DE-MALDI-MS analysis. Diagram showing the classification of proteins identified to have altered expression in the left ventricle of TPCN1 KO *vs.* WT mice by 2-DE-MALDI-MS according to their biological function using the NCBI, PantherDB and UniProt databases. Proteins were divided into 5 groups: (1) proteins associated with metabolic processes, subdivided into 4 different groups: glycolysis, lipid metabolism, tricarboxylic acid cycle and respiratory electron transport chain; (2) proteins associated with muscle contraction; (3) proteins associated with cytoskeleton organization; (4) transport proteins and (5) the chaperone protein stress-70 protein.

3.2 *Proteomics analysis of LV from TPCN1 KO mice hearts using LC-MALDI-MS*

We performed LC-MALDI-MS analysis as an alternative method to complement the 2-DE results and to saturate the cardiac proteomic map. A total of 108 proteins were identified in the 3 cardiac LV from TPCN1 KO and WT mice (supplementary table 3). A total of 22 proteins were identified in TPCN1 KO mice (supplementary table 4), 15 proteins were identified in TPCN1 WT mice (supplementary table 4), and 71 proteins were identified in common in both conditions (supplementary table 5; supplementary figure 1).

The proteins identified by LC-MALDI-MS in cardiac LV of TPCN1 KO with altered expression *vs.* WT mice (at least in 2 of the 3 mice) were further classified. According to the NCBI, PantherDB, and Uniprot databases, proteins were divided into 8 groups based on their biological function (figure 3 and supplementary table 6): (1) proteins associated with metabolic processes, subdivided into 5 different subgroups: glycolysis, lipid metabolism, TCA, respiratory electron transport chain and others; (2) muscle contraction; (3) cellular component organization or biogenesis; (4) cellular processes; (5) developmental processes; (6) immune system processes; (7) localization and (8) calcium homeostasis.

Among the proteins differentially identified in TPCN1 KO *vs.* WT mice, 15 were exclusively obtained by 2D-MALDI-MS and 11 only by LC-MALDI-MS, while 21 proteins were identified in common with the use of both techniques (supplementary figure 2 and figure 4). Thus, we confirmed that the use of LC-MALDI-MS complements the proteomic map obtained by 2D-MALDI-MS, being both

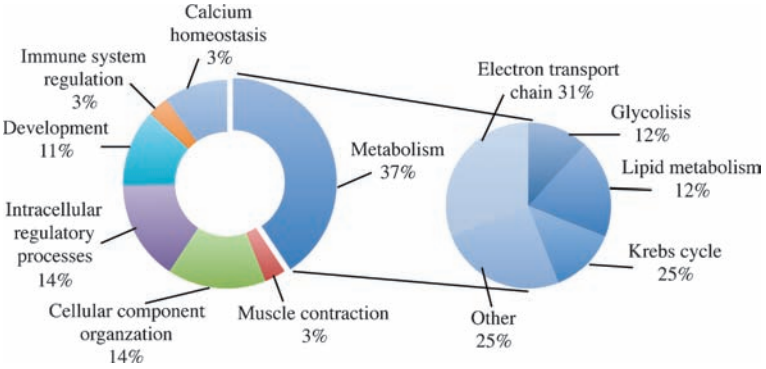

Figure 3. Results from LC-MALDI-MS analysis. Diagram showing the classification of the 22 proteins identified just in the left ventricle of TPCN1 KO mice by LC-MALDI-MS according to their biological function using the NCBI, PantherDB and UniProt databases. Proteins were divided into 8 groups based on their biological function: (1) proteins associated with metabolic processes, subdivided into 5 different groups: glycolysis, lipid metabolism, tricarboxylic acid cycle, respiratory electron transport chain and others; (2) muscle contraction; (3) cellular component organization or biogenesis; (4) cellular processes; (5) developmental processes; (6) inmune system processes; (7) localization and (8) calcium homeostasis.

techniques a good approach to achieve a better resolution of the cardiac proteome.

3.3 *Validation by Western blot of HFABP, enolase and PGK1*

As the majority of the proteins deregulated in LV cardiac tissue of TPCN1 KO mice were identified as key enzymes of metabolic regulation by 2-DE-MALDI-MS and LC-MALDI-MS (figure 4), we performed 2-DE and 1-DE Western blot analysis to validate three of them: HFABP, enolase and PGK1, which are all of them essential enzymes taking part in the first steps of fatty acid and glucose metabolism in the cytoplasmic cellular portion. We used 1-DE Western blot to identify changes in total protein expression, and 2-DE Western blot to explore possible post-translational modifications that can be unperceived in 1-DE Western blot.

HFABP plays a key role in cardiac intracellular lipid transport and mobilization, fuel selection and metabolic homeostasis regulation (Binas *et al.* 1999). 2-DE Western blot showed three modified versions of HFABP due to post-translational modifications that go to an acidic pH (theoretical HFABP pI = 6.11 ('ExPASy - Compute pI/Mw tool' n.d.)), corresponding to phosphorylated forms (Bravo *et al.* 2011) and being just one of them (spot 1) upregulated in TPCN1 KO *vs.* WT mice (F.C.=2.36±0.63, $p<0.05$, n=4) (figure 5A). As well, 1-DE Western blot for HFAPB showed increased levels of this protein in TPCN1 KO *vs.* WT mice (F.C. =2.24, $p<0.001$, n=6) (figure 5B).

The enolase catalyses the conversion of 2-phosphoglycerate to phosphoenolpyruvate during glycolysis, but it has been shown to play also an important role in other biological/pathological processes such as myogenesis (Keller *et al.* 2007), regulation of ATP-sensitive K^+ channels in cardiomyocytes (Hong *et al.* 2011) and development of ischemic (Mizukami *et al.* 2004) and hypertrophic (Zhou *et al.* 2006) cardiovascular diseases. 2-DE Western blot for enolase showed different post-translational modifications that go to a basic pH (theoretical enolase pI = 6.37 ('ExPASy - Compute pI/Mw tool' n.d.)), corresponding to dephosphorylated forms (Bravo *et al.* 2011) and being just one of them (spot 2) upregulated in TPCN1 KO *vs.* WT mice (F.C.=3.4, $p<0.01$, n=3) (figure 6A). However, 1-DE Western blot does not show differences in enolase total protein expression in TPCN1 KO *vs.* WT (figure 6B).

PGK1 catalyses the conversion of 1,3-diphosphoglycerate to 3-phosphoglycerate during glycolysis, and has it been suggested to play a role in cardiac contraction (Wang *et al.* 2008). 2-DE Western blot showed different post-translational modifications of PGK1 (theoretical PGK1 pI = 8.02 ('ExPASy - Compute pI/Mw tool' n.d.)), being just the spot 3 upregulated in TPCN1 KO *vs.* WT mice (F.C.=6.40, $p<0.01$, n=3) (figure 8A), while 1-DE Western blot does not show differences in PGK1 total protein expression in TPCN1 KO *vs.* WT mice (figure 7B).

3.4 *Effect of TPCN1 gene silencing on glucose and fatty acids uptake*

We next aimed to determine whether glucose and fatty acids uptake were affected by the absence of TPCN1. For that purpose, we performed *in vitro* experiments with siRNAs directed against the TPCN1 gene in cultured neonatal rat cardiomyocytes (TPCN1 gene expression knockdown was ≥60%, as previously described (García-Rúa *et al.* 2016) (data not shown)). Despite the fact that HFABP was found to be upregulated in mice lacking TPCN1 by 2-DE Western blot, the fatty acid uptake was unaffected by TPCN1 gene silencing in cultured neonatal rat cardiomyocytes (data not shown).

On the other hand, the downregulation of TPCN1 gene expression significantly increased 2-deoxy-D-[3H]-glucose uptake in primary cultured neonatal rat cardiomyocytes by 36.1±10.4% ($p<0.05$, n=5) (Figure 8.A), an increase similar to that induced by the positive control (100 nM insulin for 1 h, 33.3±7.2%, $p<0.01$, n=5). Analysis of confocal images of cultured neonatal rat cardiomyocytes with fluorescence-labelled glucose transporter type 4 (GLUT4, the main glucose transporter in the heart (Montessuit and Lerch 2013)) showed that TPCN1 gene silencing caused a significant translocation of GLUT4 to cell peripherals ($p<0.0001$, n=103) (figure 8B).

4. Discussion

TPCNs have been recently implicated in the pathophysiology of different metabolic disorders, including obesity (Lear *et al.* 2014), fatty liver disease (Grimm *et al.* 2014) and type 2 diabetes mellitus (T2DM) (Tsaih *et al.* 2014), which are all of them closely related to the development of cardiovascular diseases (Bang and Cho 2015; Bastien *et al.* 2013; Grundy 2015). In this work, we aimed to describe the effect of the absence of TPCN1 on cardiac metabolism regulation.

Proteomics strategies have been repeatedly followed in the last 10 years to increase the understanding of the molecular mechanisms of numerous biological systems and to identify new biomarkers of disease (Chiou and Wu 2011). Gel-based proteomics is the most popular and versatile method of global protein separation and quantification (Chevalier 2010). However, the identification of trace-level proteins, low-molecular-weight proteins, and some post-translational modified proteins is difficult due to the limitations of the 2-DE system (López 2007). In the last years, the mainstream proteomics approaches that involve 'shotgun' proteomics, in which complex protein mixtures are digested

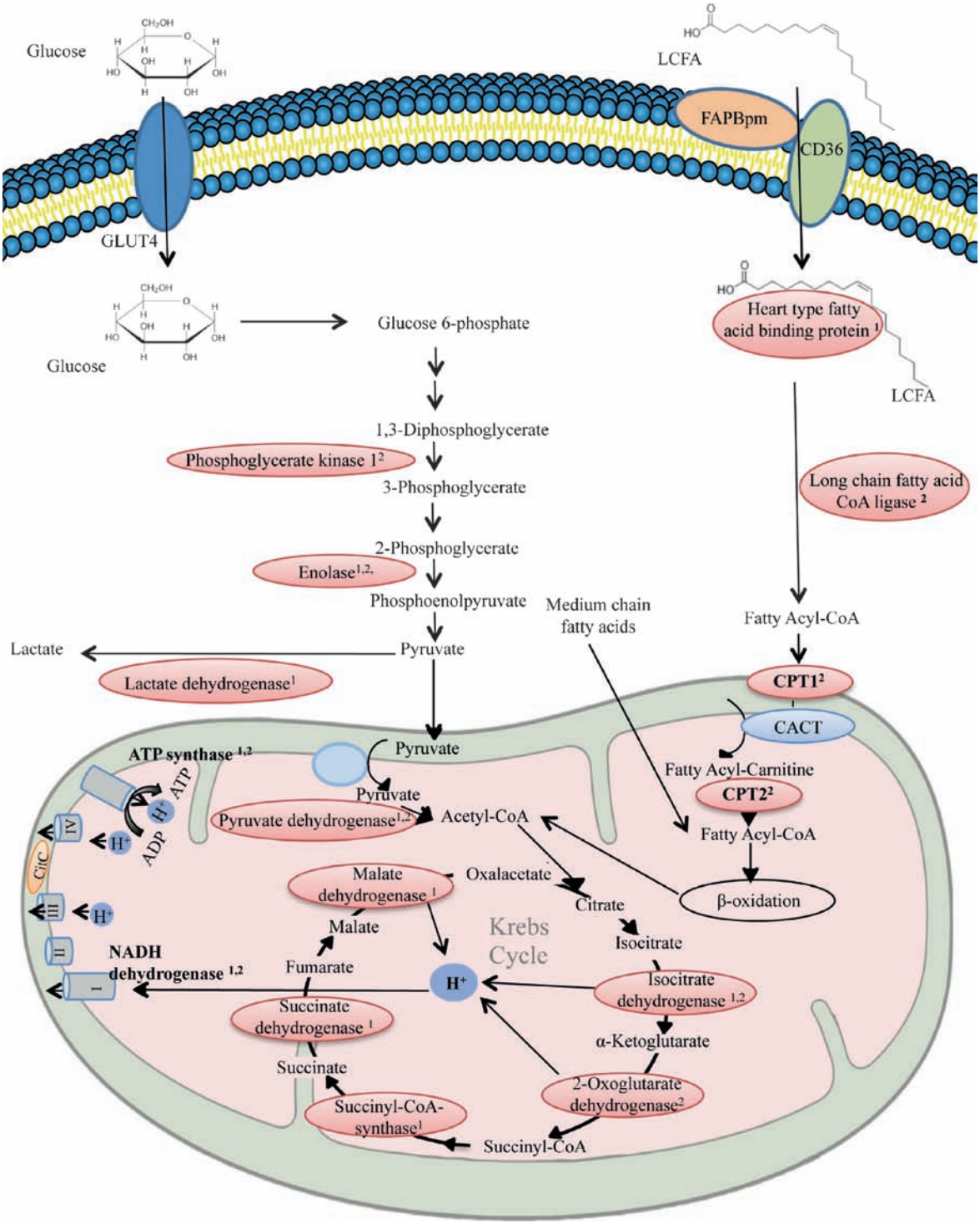

Figure 4. Schematic overview of the differentially expressed proteins associated with cardiac metabolism in the cardiomyocytes of cardiac left ventricles of TPCN1 KO mice. Proteins identified by 2-DE-MALDI-MS are represented with the number 1, and the proteins identified by LC-MALDI-MS are represented with the number 2. LCFA: long chain fatty acids, FABPpm: plasma membrane-associated fatty acid binding protein, CD36: fatty acid translocase, CPT1: carnitine palmitoyltransferase 1, CPT2: carnitine palmitoyltransferase 2, CACT: carnitine/acylcarnitine translocase, CitC: cytochrome C.

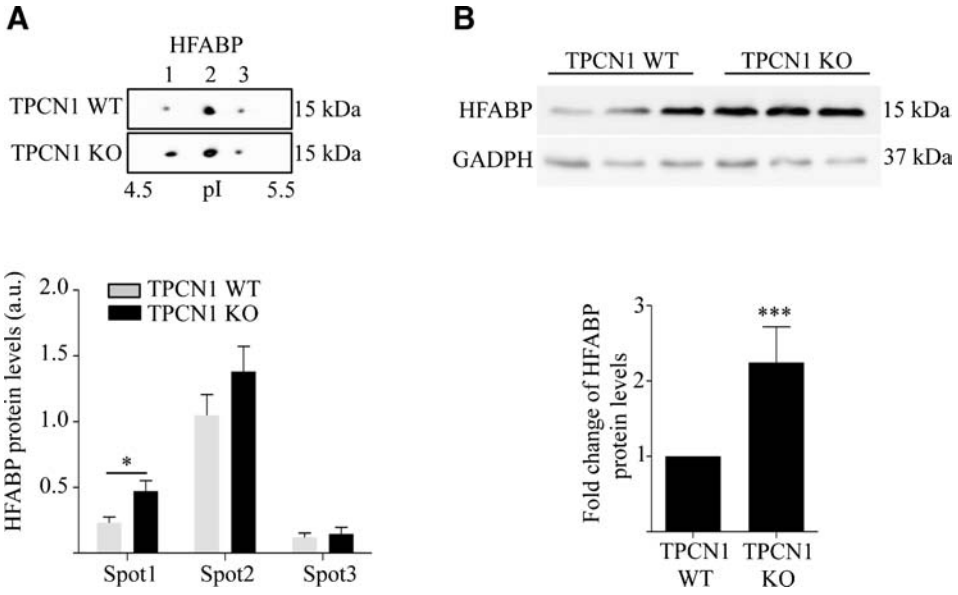

Figure 5. Western blot analysis of HFABP. (**A**) 2-DE Western blot analysis of the protein samples obtained from the cardiac left ventricles of TPCN1 KO and WT mice. There were found three modified versions of HFABP due to post-translational modifications that go to an acidic pH (theoretical HFABP pI = 6.11 ('ExPASy - Compute pI/Mw tool' n.d.)), corresponding to phosphorylated forms (Bravo *et al.* 2011) and being just one of them (spot 1) upregulated in TPCN1 KO *vs.* WT mice (F.C.=2.36±0.63, $p<0.05$, n=4). (**B**) 1-DE Western blot of the protein samples obtained from the cardiac left ventricles of TPCN1 KO and WT mice. There were found increased levels of HFABP in TPCN1 KO *vs.* WT mice (F.C.=2.24, $p<0.001$, n=6). *$p<0.05$, ***$p<0.001$, a.u: arbitrary units.

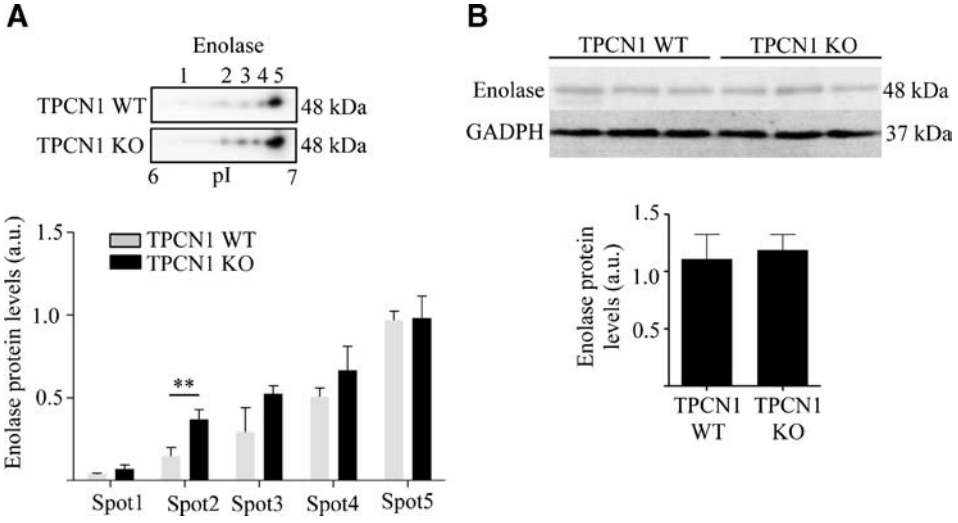

Figure 6. Western blot analysis of enolase. (**A**) 2-DE Western blot analysis of the protein samples obtained from the cardiac left ventricles of TPCN1 KO and WT mice. There were found 5 different post-translational modifications that go to a basic pH (theoretical enolase pI = 6.37 ('ExPASy - Compute pI/Mw tool' n.d.)), corresponding to dephosphorylated forms (Bravo *et al.* 2011) and being just one of them (spot 2) upregulated in TPCN1 KO *vs.* WT mice (F.C.=3.4, $p<0.01$, n=3). (**B**) 1-DE Western blot analysis of the protein samples obtained from the cardiac left ventricles of TPCN1 KO and WT mice. There were no changes found in total enolase protein levels between both mice (n= 4). **$p<0.01$, a.u: arbitrary units.

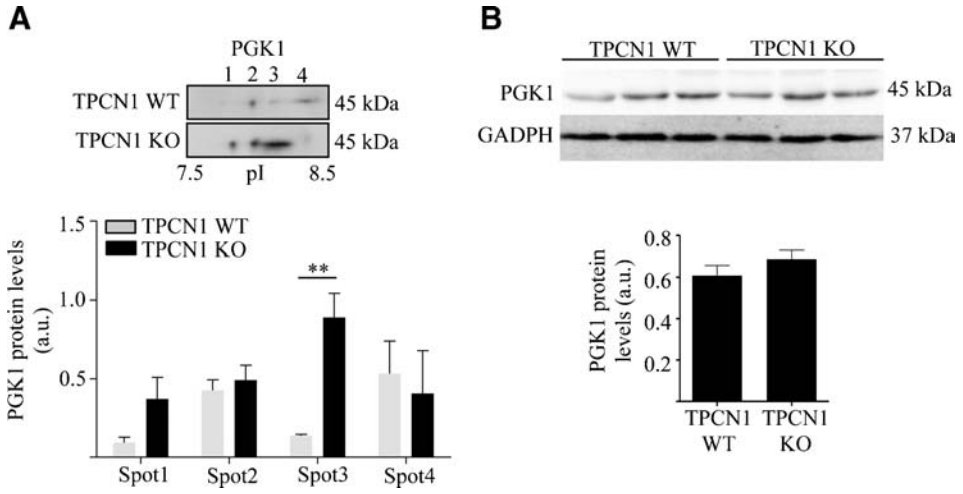

Figure 7. Western blot analysis of PGK1. (**A**) 2-DE Western blot analysis of the protein samples obtained from the cardiac left ventricles of TPCN1 KO and WT mice. There were found 4 post-translational modifications of PGK1 (theoretical PGK1 pI = 8.02 ('ExPASy - Compute pI/Mw tool' n.d.)), being just the spot 3 upregulated in TPCN1 KO *vs.* WT mice (F.C.=6.40, $p<0.01$, n=3). (**B**) 1-DE Western blot analysis of the protein samples obtained from the cardiac left ventricles of TPCN1 KO and WT mice. There were no changes found in total PGK1 protein levels between both mice (n= 4). **$p<0.01$, a.u: arbitrary units.

into peptides, which are subsequently separated through reverse-phase liquid chromatography (LC) and analysed using mass spectrometry (MS), have been widely used and improved (Roca-Rivada *et al.* 2015; Tuli and Ressom 2009). This technique resolves the peptides prior to mass spectrometry analysis, thus dramatically increasing the number of protein identifications and sequence coverage in complex samples (Faça *et al.* 2014). LC/MS has good selectivity and sensitivity and is a fast and accurate bioanalytical tool for proteomics (Zhang *et al.* 2010). Thus, this technology has been used for the molecular characterization of different human diseases, such as myocardial infarction (Alonso-Orgaz *et al.* 2014), obesity-induced diabetes (Bollineni *et al.* 2014) and biomarker cancer discovery (Shevchenko *et al.* 2013; Bergamini *et al.* 2014). In our study, we confirmed that LC-MALDI-MS not only represent a complementary method to validate the results from 2-DE-MALDI-MS, but also provides additional information missed by 2-DE, so that the combination of both techniques represent an appropriate method to increase our cardiac proteomic map.

To determine the possible role of TPCN1 in cardiac metabolism, we used these two proteomics techniques in LV of TPCN1 KO *vs.* WT mice, facilitating the construction of a 2-DE map of the TPCN1 KO *vs*. WT mice in cardiac tissue and the identification of altered proteins. This approach showed differential expression of key proteins implicated in energy metabolism regulation between both mice. Using 2-DE-MALDI-MS, we identified in TPCN1 KO *vs.* WT mice 5 proteins upregulated which were involved in the regulation of the glycolytic pathway (beta-enolase, gamma-enolase, pyruvate dehydrogenase E1 component and L-lactate dehydrogenase B chain) (supplementary table 2). Also, using LC-MALDI-MS, we identified 22 proteins in TPCN1 KO mice, 2 of which were also key metabolic enzymes of glycolysis (alpha-enolase and PGK1) (supplementary table 4). The validation of enolase and PGK1 by 2-DE-Western blot confirmed the increased expression of one of the post-translational modifications of these proteins in cardiac LV tissue of TPCN1 KO *vs.* WT mice, while 1-DE Western blot did not show changes in total protein levels, which reveals the importance of the use of 2-DE proteomics approaches. TPCN1 gene silencing in neonatal rat cardiomyocytes induced an increase in glucose uptake and GLUT4 mobilization to cell peripherals, supporting the possible role of TPCN1 in glycolysis regulation, as suggested by proteomics assays.

As the major consumer of energy in the body, the heart requires large amounts of adenosine triphosphate (ATP) to sustain contractile function (Lopaschuk *et al.* 2010). It is widely accepted that fatty acids are the main energy substrates used by the normal adult myocardium, providing ~70% of ATP (Lopaschuk *et al.* 2010). However, the heart is highly flexible in using other substrates depending on its patho/physiological conditions and on the energetic context, being able to use carbohydrates, lipids, amino acids or ketone bodies for ATP generation in the mitochondria, a concept known as metabolic flexibility of the heart (Kolwicz *et al.* 2013). Although the normal heart preferentially oxidizes fatty acids, the increased energy requirements of hearts subjected to high workload are met by the carbohydrate

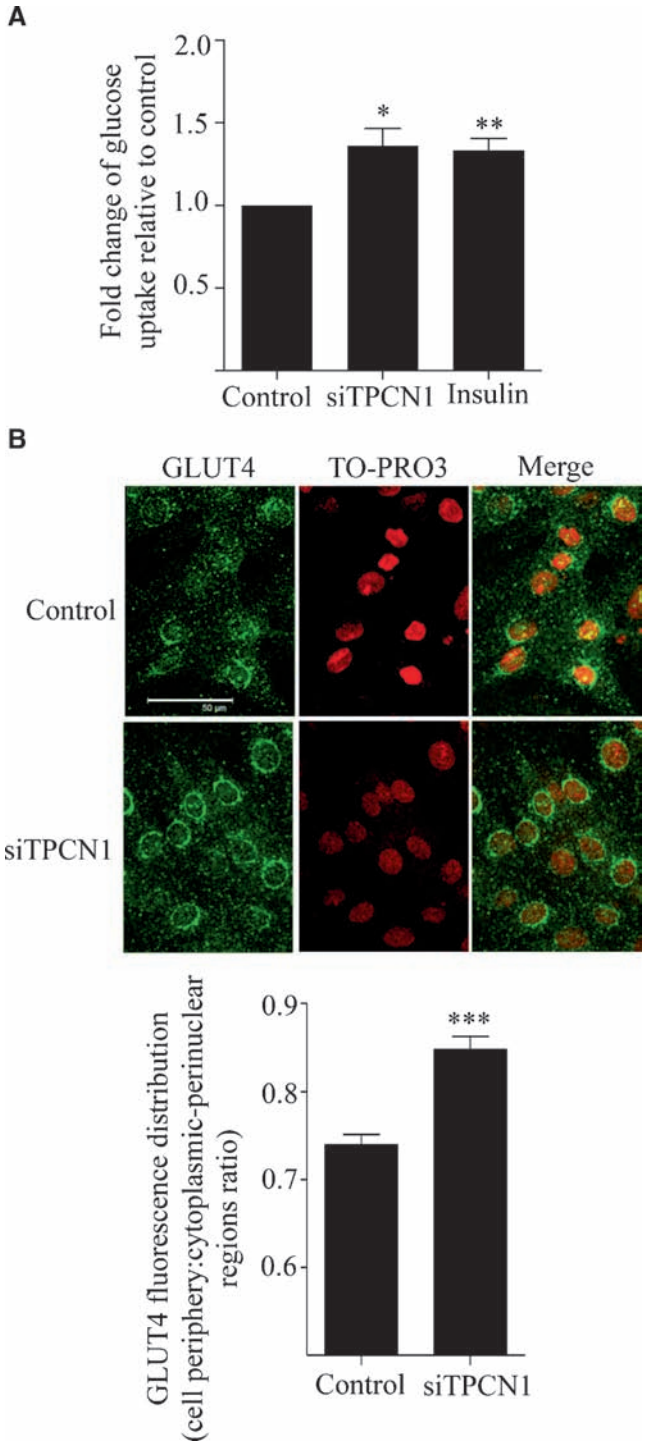

Figure 8. Effect of TPCN1 gene silencing on glucose uptake and GLUT4 mobilization. (**A**) Uptake of 2-deoxy-D-[3H]-glucose by neonatal rat cardiomyocytes after 48 h post-transfection with TPCN1 siRNA relative to untransfected controls. Downregulation of TPCN1 gene expression significantly increased 2-deoxy-D-[3H]-glucose uptake in primary cultured neonatal rat cardiomyocytes by 36.1±10.4% ($p<0.05$, n=5), an increase similar to that induced by the positive control (100 nM insulin for 1 h, 33.3±7.2%, $p<0.01$, n=5). (**B**) Confocal microscopy analysis of glucose transporter GLUT4 translocation to the cell peripherals in response to TPCN1 gene silencing in neonatal rat cardiomyocytes. TPCN1 gene silencing caused a significant translocation of GLUT4 to cell peripherals by 17.70±2.75% ($p<0.0001$, n=103), decreasing its amount in the cytoplasmic perinuclear area of the cardiomyocytes. Scale bar corresponds to 50 μm. TO-PRO 3: nuclear staining. n=108, *$p<0.05$, **$p<0.01$, ***$p<0.001$.

oxidation (Sen *et al.* 2013), and accelerated glycolysis has been suggested to potentially stimulate muscle glucose uptake (Wasserman *et al.* 2011). Our results are the first showing an alteration in glucose uptake and metabolism in heart tissue due to the absence of TPCN1. In this line, several studies have suggested an interplay between different ion channels activity and glucose metabolism in cardiomyocytes: the calcium-permeable cation channel TRPM2 (transient receptor potential cation channel, subfamily M, member 2) deficiency has been shown to enhance insulin sensitivity in diet-induced obese mice, partially reflecting a significant increase in skeletal muscle and cardiac glucose metabolism (Zhang *et al.* 2012); also, it has been shown that the inhibition of a key enzyme of glucose catabolism, glucose-6-phosphate dehydrogenase, can reduce the activity of L-type Ca^{2+} channels (Rawat *et al.* 2012); and it has also been demonstrated that the increase of intracellular Ca^{2+} levels can increase the insulin-stimulated glucose transporter 4 (GLUT4) expression in L6 muscle cells (Wright 2007); and, finally, the Ca^{2+} channel inositol 1,4,5-triphosphate (IP3) receptor is required for GLUT4 translocation and glucose uptake in cardiomyocytes (Contreras-Ferrat *et al.* 2010).

TPCNs regulation by NAADP has been suggested to participate in the control of circulating glucose levels through the control of glucose-induced Ca^{2+} signals in pancreatic β-cells that induce insulin release (Arredouani *et al.* 2015), and it was suggested that they could act as nutrient sensors linked to mTOR action and ATP levels (Cang *et al.* 2013; Jha *et al.* 2014; Lin *et al.* 2015). So that, it seems reasonable that they could also participate in the regulation of cardiac metabolism. In fact, our group has previously demonstrated in cultured cardiomyocytes that starvation induced a significant increase in TPCN1 and TPCN2 transcript and protein levels that paralleled an increase in autophagy, and that siRNA depletion of TPCN2 alone or together with TPCN1 impairs the autophagic flux both under basal conditions and in response to serum starvation, suggesting that TPCNs are regulated by nutrient status at cardiac level and that under conditions of severe energy depletion, changes in the autophagic flux occur either when TPCNs are down-regulated (García-Rúa *et al.* 2016). As well, we have also demonstrated in a previous work that TPCN1 and TPCN2 gene expression is upregulated in LV tissue of patients with heart failure (Garcia-Rua *et al.* 2012), which is a pathological state characterised by several metabolic alterations, ranging from changes in substrate use to mitochondrial dysfunction, ultimately resulting in ATP deficiency and impaired contractility (Wang *et al.* 2014).

Regarding lipid metabolism, using 2-DE-MALDI-MS, we identified in TPCN1 KO *vs.* WT mice a differential pattern of protein expression of apolipoprotin AI and HFABP (supplementary tables 1 and 2). Due to the importance of HFABP in cardiac intracellular lipid transport and mobilization, fuel selection and metabolic homeostasis regulation (Binas *et al.* 1999), we validated this result by 2-DE Western blot, identifying three spots, one of them upregulated in TPCN1 KO mice, and observing an increase in total protein levels by 1-DE Western blot. This result could suggest that the absence of TPCN1 might induce changes in myocardial lipid metabolism. However, we did not observe any change in BODIPY-labelled fatty acid uptake by neonatal rat cardiomyocytes when the TPCN1 gene expression was silenced (data not shown). This technique was used as a first approximation to the study of the physiological relevance of TPCN1 on lipid metabolism at cardiac level. The lack of changes observed in the BODIPY-labelled fatty acids uptake in cultured cardiomyocytes do not exclude that the alteration in HFABP revealed by the proteomic study in TPCN1 KO mice could have physiological consequences on cardiomyocyte lipid metabolism. These results could be due to (1) HFABP is involved not only in long chain fatty acids uptake *de novo* by the cells but also in the intracellular metabolism and/or transport of long-chain fatty acids (Binas *et al.* 1999), and (2) *in vivo* KO animals and *in vitro* knock-down experiments are two experimental approaches that have different degree, timing and characteristics of gene silencing, and that have been shown to often lead to different phenotypes (Stainier *et al.* 2015).

Using LC-MALDI-MS, we identified 22 proteins in TPCN1 KO *vs.* WT mice, 3 of which were also related to lipid metabolism (carnitine O-palmitoyltransferase 2, long-chain-fatty-acid-CoA ligase 1 and trifunctional enzyme subunit beta) (supplementary table 4). Some of these enzymes are directly implicated in lipid catabolism, being the fatty acid entry into the mitochondria the main checkpoint, a process regulated by Carnitine O-palmitoyltransferase 1 (CPT1) through the conversion of long-chain acyl CoA to long-chain acylcarnitine (LCA) for subsequent transport to the mitochondria (Lopaschuk *et al.* 2010). Once in the mitochondrial matrix, LCA is converted back to long-chain acyl CoA by CPT2 (identified in TPCN1 KO mice), a 70-kDa enzyme located in the inner mitochondrial membrane (Lopaschuk *et al.* 2010). Therefore, these results suggest that TPCNs might play a role in lipid metabolism at cardiac level. Recently, it has been proposed that the double KO mice for TPCN1 and TPCN2 show mature-onset obesity due to reduced lipid availability and use at systemic level (Lear *et al.* 2014), and that the TPCN2 KO mice have higher susceptibility to develop fatty liver disease due to a dysfunction of the endolysosomal degradation pathway most likely on the

level of late endosome to lysosome fusion (Grimm *et al.* 2014), raising the possibility of TPCNs participation in lipid management. Consistently, it has been proposed that other ion channels, such as the mammalian transient receptor potential canonical (TRPC), a family of calcium-permeable channels (Venkatachalam and Montell 2007), could act as lipid-sensing receptors (Beech *et al.* 2009).

In our study, we identified in cardiac tissue a different expression pattern of several key enzymes of the tricarboxylic acid cycle (TCA) (succinyl-CoA ligase [ADP-forming] subunit beta, isocitrate dehydrogenase [NAD] subunit and malate dehydrogenase) and of the respiratory electron transport chain (cytochrome b-c1 complex subunit l, ATP synthase subunit beta, succinate dehydrogenase [ubiquinone] flavoprotein subunit, NADH dehydrogenase [ubiquinone] iron-sulphur protein 3, ATP synthase-coupling factor 6, NADH dehydrogenase [ubiquinone] flavoprotein 2) in TPCN1 KO *vs*. WT mice by 2-DE-MALDI-MS (supplementary table 2). LC-MALDI-MS analysis reinforced these results identifying proteins related to TCA (2-Oxoglutarate dehydrogenase and dihydrolipoyl dehydrogenase), and to the respiratory electron transport chain (ATP synthase subunit O, NADH dehydrogenase [ubiquinone] iron-sulphur protein 2 and NADH-ubiquinone oxidoreductase 75 kDa subunit, ATP synthase subunit gamma) in TPCN1 KO *vs.* WT mice (supplementary table 4). However, it is important to note that the absence of protein identification by LC-MALDI-MS do not exclude the possibility of protein presence in the sample, so that when proteins are expressed in low quantity or are highly hydrophilic/hydrophobic, they can not be well detected by this technique. In summary, all these results infer the possible involvement of TPCN1 in the regulation of ATP synthesis (a common end point of both glucose and fatty acid metabolism (Osellame *et al.* 2012)) at cardiac level.

On the whole, the results of our work provide an overview of candidate proteins involved in metabolic regulation that have altered expression due to the absence of TPCN1, and confirm a potential role for TPCNs in cardiac glucose uptake. However, additional studies are needed to better understand the mechanisms linking endolysosomal TPCNs to metabolic homeostasis in cardiac cells.

5. Conclusion

The present study is the first to characterize a differential pattern of expression of key enzymes related to glucose and fatty acid metabolism in cardiac left ventricles of TPCN1 KO mice *vs.* WT mice by the use of a proteomic approach that combines 2-DE-MALDI-MS and LC-MALDI-MS, increasing the cardiac proteomic map. These results were accompanied by a concurrent increase in glucose uptake in the primary culture of neonatal rat cardiomyocytes, where TPCN1 gene expression was downregulated, suggesting a possible association between TPCNs and cardiac metabolism regulation. Additional future works should be performed in order to assess the specific intracellular signalling cascades that link TPCN1 to cardiac metabolic regulation.

Acknowledgements

Funding was from the cardiovascular research network (RIC) of the Spanish thematic cooperative research networks in health (RETICs) associated with the Carlos III Health Institute and European Regional Development Fund (ERDF). The funding source was not involved in the conduct of the research and/or preparation of the article, or in the decision to submit the article for publication.

References

Aley PK, Mikolajczyk AM, Munz B, Churchill GC, Galione A and Berger F 2010 Nicotinic acid adenine dinucleotide phosphate regulates skeletal muscle differentiation via action at two-pore channels. *Proc. Natl. Acad. Sci. USA* **107** 19927–19932

Alonso-Orgaz S, Moreno-Luna R, López JA, Gil-Dones F, Padial LR, Moreu J, de la Cuesta F and Barderas MG 2014 Proteomic characterization of human coronary thrombus in patients with ST-segment elevation acute myocardial infarction. *J. Proteome.* **109** 368–381

Arndt L, Castonguay J, Arlt E, Meyer D, Hassan S, Borth H, Zierler S, Wennemuth G, *et al*. 2014 NAADP and the two-pore channel protein 1 participate in the acrosome reaction in mammalian spermatozoa. *Mol. Biol. Cell* **25** 948–964

Arredouani A, Ruas M, Collins SC, Parkesh R, Clough F, Pillinger T, Coltart G, Rietdorf K, *et al*. 2015 Nicotinic Acid Adenine Dinucleotide Phosphate (NAADP) and Endolysosomal Two-pore Channels Modulate Membrane Excitability and Stimulus-Secretion Coupling in Mouse Pancreatic Beta Cells. *J. Biol. Chem.* **290** 21376–21392

Bang KB and Cho YK 2015 Comorbidities and metabolic derangement of NAFLD. *J. Lifestyle Med.* **5** 7–13

Bastien M, Poirier P, Lemieux I and Després J-P 2013 Overview of epidemiology and contribution of obesity to cardiovascular disease. *Prog. Cardiovasc. Dis.* **56** 369–381

Beech DJ, Bahnasi YM, Dedman AM and Al-Shawaf E 2009 TRPC channel lipid specificity and mechanisms of lipid regulation. *Cell Calcium* **45** 583–588

Bergamini S, Bellei E, Reggiani Bonetti L, Monari E, Cuoghi A, Borelli F, Sighinolfi MC, Bianchi G, *et al*. 2014 Inflammation:

an important parameter in the search of prostate cancer biomarkers. *Proteome Sci.* **12** 32

Binas B, Danneberg H, McWhir J, Mullins L and Clark AJ 1999 Requirement for the heart-type fatty acid binding protein in cardiac fatty acid utilization. *FASEB J.* **13** 805–812

Bollineni RC, Fedorova M, Blüher M and Hoffmann R 2014 Carbonylated plasma proteins as potential biomarkers of obesity induced type 2 diabetes mellitus. *J. Proteome Res.* **13** 5081–5093

Bonzon-Kulichenko E, Pérez-Hernández D, Núñez E, Martínez-Acedo P, Navarro P, Trevisan-Herraz M, Ramos Mdel C, Sierra S, *et al*. 2011 A robust method for quantitative high-throughput analysis of proteomes by 18O labeling. *Mol. Cell Proteomics.* **10** M110.003335

Brailoiu E, Churamani D, Cai X, Schrlau MG, Brailoiu GC, Gao X, Hooper R, Boulware MJ, *et al*. 2009 Essential requirement for two-pore channel 1 in NAADP-mediated calcium signaling. *J. Cell Biol.* **186** 201–209

Bravo SB, Caminos JE, González CR, Vázquez MJ, Garcés MF, Cepeda LA, García-Rendueles MER, Iglesias-Gamarra A, *et al*. 2011 Leptin and fasting regulate rat gastric glucose-regulated protein 58. *Int. J. Pept.* **2011** 969818

Calcraft PJ, Ruas M, Pan Z, Cheng X, Arredouani A, Hao X, Tang J, Rietdorf K, *et al*. 2009 NAADP mobilizes calcium from acidic organelles through two-pore channels. *Nature* **459** 596–600

Cang C, Zhou Y, Navarro B, Seo Y, Aranda K, Shi L, Battaglia-Hsu S, Nissim I, *et al*. 2013 mTOR regulates lysosomal ATP-sensitive two-pore Na(+) channels to adapt to metabolic state. *Cell* **152** 778–790

Chevalier F 2010 Highlights on the capacities of 'Gel-based' proteomics. *Proteome Sci.* **8** 23

Chiou S-H and Wu C-Y 2011 Clinical proteomics: current status, challenges, and future perspectives. *Kaohsiung J. Med. Sci.* **27** 1–14

Contreras-Ferrat AE, Toro B, Bravo R, Parra V, Vásquez C, Ibarra C, Mears D, Chiong M, *et al*. 2010 An inositol 1,4,5-triphosphate (IP3)-IP3 receptor pathway is required for insulin-stimulated glucose transporter 4 translocation and glucose uptake in cardiomyocytes. *Endocrinology* **151** 4665–4677

Dionisio N, Albarrán L, López JJ, Berna-Erro A, Salido GM, Bobe R and Rosado JA 2011 Acidic NAADP-releasable Ca(2+) compartments in the megakaryoblastic cell line MEG01. *Biochim. Biophys. Acta.* **1813** 1483–1494

ExPASy - Compute pI/Mw tool [WWW Document], n.d. URL http://web.expasy.org/compute_pi/ (accessed 2.2.16)

Faça VM, Palma CS, Albuquerque D, Canchaya GNS, Grassi ML, Epifânio VL and De OEB 2014 Shotgun. *Proteomics.* **1156** 323–335

Favia A, Desideri M, Gambara G, D'Alessio A, Ruas M, Esposito B, Del Bufalo D, Parrington J, *et al*. 2014 VEGF-induced neoangiogenesis is mediated by NAADP and two-pore channel-2-dependent Ca2+ signaling. *Proc. Natl. Acad. Sci. USA* **111** E4706–E4715

Feijóo-Bandín S, Rodríguez-Penas D, García-Rúa V, Mosquera-Leal A, Otero MF, Pereira E, Rubio J, Martínez I, *et al*. 2013 Nesfatin-1 in human and murine cardiomyocytes: synthesis, secretion, and mobilization of GLUT-4. *Endocrinology* **154** 4757–4767

Garcia-Rua V, Otero MF, Lear PV, Rodriguez-Penas D, Feijoo-Bandin S, Noguera-Moreno T, Calaza M, Alvarez-Barredo M, *et al*. 2012 Increased expression of fatty-acid and calcium metabolism genes in failing human heart. *PLoS One* **7** 5–7

García-Rúa V, Feijóo-Bandín S, Rodríguez-Penas D, Mosquera-Leal A, Abu-Assi E, Beiras A, Seoane L, Lear P, *et al*. 2016 Endolysosomal two-pore channels regulate autophagy in cardiomyocytes. *J. Physiol.* **594** 3061–3077

González-Juanatey JR, Iglesias MJ, Alcaide C, Piñeiro R and Lago F 2003 Doxazosin induces apoptosis in cardiomyocytes cultured in vitro by a mechanism that is independent of alpha1-adrenergic blockade. *Circulation* **107** 127–131

Grimm C, Holdt LM, Chen C-C, Hassan S, Müller C, Jörs S, Cuny H, Kissing S, *et al*. 2014 High susceptibility to fatty liver disease in two-pore channel 2-deficient mice. *Nat. Commun.* **5** 4699

Grundy SM 2015 Metabolic syndrome update. *Trends Cardiovasc. Med.*

Hong M, Kefaloyianni E, Bao L, Malester B, Delaroche D, Neubert TA and Coetzee WA 2011 Cardiac ATP-sensitive K+ channel associates with the glycolytic enzyme complex. *FASEB J.* **25** 2456–2467

Horton JS, Wakano CT, Speck M and Stokes AJ 2015 Two-pore channel 1 interacts with citron kinase, regulating completion of cytokinesis. *Channels (Austin).* **9** 21–29

Ishibashi K, Suzuki M and Imai M 2000 Molecular cloning of a novel form (two-repeat) protein related to voltage-gated sodium and calcium channels. *Biochem. Biophys. Res. Commun.* **270** 370–376

Jha A, Ahuja M, Patel S, Brailoiu E and Muallem S 2014 Convergent regulation of the lysosomal two-pore channel-2 by Mg2+, NAADP, PI(3,5)P2 and multiple protein kinases. *EMBO J.* **33** 501–511

Keller A, Peltzer J, Carpentier G, Horváth I, Oláh J, Duchesnay A, Orosz F and Ovádi J 2007 Interactions of enolase isoforms with tubulin and microtubules during myogenesis. *Biochim. Biophys. Acta.* **1770** 919–926

Kolwicz SC, Purohit S and Tian R 2013 Cardiac metabolism and its interactions with contraction, growth, and survival of cardiomyocytes. *Circ. Res.* **113** 603–616

Lear PV, González-Touceda D, Porteiro Couto B, Viaño P, Guymer V, Remzova E, Tunn R, Chalasani A, *et al*. 2014 Absence of intracellular ion channels TPC1 and 2 leads to mature-onset obesity in male mice, due to impaired lipid availability for thermogenesis in brown adipose tissue. *Endocrinology* **156**, en20141766

Lin P-H, Duann P, Komazaki S, Park KH, Li H, Sun M, Sermersheim M, Gumpper K, *et al*. 2015 Lysosomal two-pore channel subtype 2 (TPC2) regulates skeletal muscle autophagic signaling. *J. Biol. Chem.* **290** 3377–3389

Lopaschuk GD, Ussher JR, Folmes CDL, Jaswal JS and Stanley WC 2010 Myocardial fatty acid metabolism in health and disease. *Physiol. Rev.* **90** 207–258

López JL 2007 Two-dimensional electrophoresis in proteome expression analysis. *J. Chromatogr. B Anal. Technol. Biomed. Life Sci.* **849** 190–202

Lu Y, Hao B-X, Graeff R, Wong CWM, Wu W-T and Yue J 2013 Two pore channel 2 (TPC2) inhibits autophagosomal-lysosomal fusion by alkalinizing lysosomal pH. *J. Biol. Chem.* **288** 24247–24263

Mizukami Y, Iwamatsu A, Aki T, Kimura M, Nakamura K, Nao T, Okusa T, Matsuzaki M, *et al*. 2004 ERK1/2 regulates intracellular ATP levels through alpha-enolase expression in cardiomyocytes exposed to ischemic hypoxia and reoxygenation. *J. Biol. Chem.* **279** 50120–50131

Montessuit C and Lerch R 2013 Regulation and dysregulation of glucose transport in cardiomyocytes. *Biochim. Biophys. Acta.* **1833** 848–856

Notomi T, Ezura Y and Noda M 2012 Identification of two-pore channel 2 as a novel regulator of osteoclastogenesis. *J. Biol. Chem.* **287** 35057–35064

Osellame LD, Blacker TS and Duchen MR 2012 Cellular and molecular mechanisms of mitochondrial function. *Best Pract. Res. Clin. Endocrinol. Metab.* **26** 711–723

Parrington J and Tunn R 2014 Ca(2+) signals, NAADP and two-pore channels: role in cellular differentiation. *Acta Physiol (Oxford).* **211** 285–296

Peiter E, Maathuis FJM, Mills LN, Knight H, Pelloux J, Hetherington AM and Sanders D 2005 The vacuolar Ca2+-activated channel TPC1 regulates germination and stomatal movement. *Nature* **434** 404–408

Pereira GJS, Hirata H, do Carmo LG, Stilhano RS, Ureshino RP, Medaglia NC, Han SW, Churchill G, *et al*. 2014 NAADP-sensitive two-pore channels are present and functional in gastric smooth muscle cells. *Cell Calcium* **56** 51–58

Perez-Hernandez D, Gutiérrez-Vázquez C, Jorge I, López-Martín S, Ursa A, Sánchez-Madrid F, Vázquez J and Yáñez-Mó M 2013 The intracellular interactome of tetraspanin-enriched microdomains reveals their function as sorting machineries toward exosomes. *J. Biol. Chem.* **288** 11649–11661

Rawat DK, Hecker P, Watanabe M, Chettimada S, Levy RJ, Okada T, Edwards JG and Gupte SA 2012 Glucose-6-phosphate dehydrogenase and NADPH redox regulates cardiac myocyte L-type calcium channel activity and myocardial contractile function. *PLoS One* **7** 1–10

Roca-Rivada A, Belen Bravo S, Pérez-Sotelo D, Alonso J, Castro AI, Baamonde I, Baltar J, Casanueva FF, *et al*. 2015 CILAIR-based secretome analysis of obese visceral and subcutaneous adipose tissues reveals distinctive ECM remodeling and inflammation mediators. *Sci. Rep.* **5** 12214

Ruas M, Rietdorf K, Arredouani A, Davis LC, Lloyd-Evans E, Koegel H, Funnell TM, Morgan AJ, *et al*. 2010 Purified TPC isoforms form NAADP receptors with distinct roles for Ca2+ signaling and endolysosomal trafficking. *Curr. Biol.* **20** 703–709

Ruas M, Chuang K-T, Davis LC, Al-Douri A, Tynan PW, Tunn R, Teboul L, Galione A, *et al*. 2014 TPC1 has two variant isoforms, and their removal has different effects on endolysosomal functions compared to loss of TPC2. *Mol. Cell Biol.* **34** 3981–3992

Sen S, Kundu BK, Wu HC-J, Hashmi SS, Guthrie P, Locke LW, Roy RJ, Matherne GP, *et al*. 2013 Glucose regulation of load-induced mTOR signaling and ER stress in mammalian heart. *J. Am. Heart Assoc.* **2**, e004796

Shevchenko A, Wilm M, Vorm O and Mann M 1996 Mass spectrometric sequencing of proteins silver-stained polyacrylamide gels. *Anal. Chem.* **68** 850–858

Shevchenko VE, Kovalev SV, Arnotskaya NE, Zborovskaya IB, Akhmedov BB, Polotskii BE, Kostin AU, Moukeria AF, *et al*. 2013 Human blood plasma proteome mapping for search of potential markers of the lung squamous cell carcinoma. *Eur. J. Mass Spectrom. (Chichester, Eng.).* **19** 123–133

Stainier DYR, Kontarakis Z and Rossi A 2015 Making sense of anti-sense data. *Dev. Cell* **32** 7–8

Terman A and Brunk UT 2005 Autophagy in cardiac myocyte homeostasis, aging, and pathology. *Cardiovasc. Res.* **68** 355–365

Tsaih S-W, Holl K, Jia S, Kaldunski M, Tschannen M, He H, Andrae JW, Li S-H, *et al*. 2014 Identification of a novel gene for diabetic traits in rats, mice, and humans. *Genetics* **198** 17–29

Tugba Durlu-Kandilci N, Ruas M, Chuang K-T, Brading A, Parrington J and Galione A 2010 TPC2 proteins mediate nicotinic acid adenine dinucleotide phosphate (NAADP)- and agonist-evoked contractions of smooth muscle. *J. Biol. Chem.* **285** 24925–24932

Tuli L and Ressom HW 2009 LC-MS based detection of differential protein expression. *J. Proteomics Bioinform.* **2** 416–438

Venkatachalam K and Montell C 2007 TRP channels. *Annu. Rev. Biochem.* **76** 387–417

Wang R, Liang J, Jiang H, Qin L-J and Yang H-T 2008 Promoter-dependent EGFP expression during embryonic stem cell propagation and differentiation. *Stem Cells Dev.* **17** 279–289

Wang X, Zhang X, Dong X-P, Samie M, Li X, Cheng X, Goschka A, Shen D, *et al*. 2012 TPC proteins are phosphoinositide- activated sodium-selective ion channels in endosomes and lysosomes. *Cell* **151** 372–383

Wang ZV, Li DL and Hill JA 2014 Heart failure and loss of metabolic control. *J. Cardiovasc. Pharmacol.* **63** 302–313

Wasserman DH, Kang L, Ayala JE, Fueger PT and Lee-Young RS 2011 The physiological regulation of glucose flux into muscle in vivo. *J. Exp. Biol.* **214** 254–262

Wright DC 2007 Mechanisms of calcium-induced mitochondrial biogenesis and GLUT4 synthesis. *Appl. Physiol. Nutr. Metab.* **32** 840–845

Zhang X, Fang A, Riley CP, Wang M, Regnier FE and Buck C 2010 Multi-dimensional liquid chromatography in proteomics–a review. *Anal. Chim. Acta.* **664** 101–113

Zhang Z, Zhang W, Jung DY, Ko HJ, Lee Y, Friedline RH, Lee E, Jun J, *et al*. 2012 TRPM2 Ca2+ channel regulates energy balance and glucose metabolism. *Am. J. Physiol. Endocrinol. Metab.* **302** E807–E816

Zhang Z-H, Lu Y-Y and Yue J 2013 Two pore channel 2 differentially modulates neural differentiation of mouse embryonic stem cells. *PLoS One* **8** e66077

Zhou S-G, Zhou S-F, Huang H-Q, Chen J-W, Huang M and Liu P-Q 2006 Proteomic analysis of hypertrophied myocardial

protein patterns in renovascularly hypertensive and spontaneously hypertensive rats. *J. Proteome Res.* **5** 2901–2908

Zhu MX, Ma J, Parrington J, Calcraft PJ, Galione A and Evans AM 2010 Calcium signaling via two-pore channels: local or global, that is the question. *Am. J. Physiol. Cell Physiol.* **298** C430–C441

Zong X, Schieder M, Cuny H, Fenske S, Gruner C, Rötzer K, Griesbeck O, Harz H, *et al*. 2009 The two-pore channel TPCN2 mediates NAADP-dependent Ca2+-release from lysosomal stores. *Pflugers Arch. - Eur. J. Physiol.* **458** 891–899

MS received 07 April 2016; accepted 15 September 2016

Corresponding editor: Sudha Bhattacharya